JPET Fast Forward. Published on January 14, 2020 as DOI: 10.1124/jpet.119.262865
This article has not been copyedited and formatted. The final version may differ from this version.

Detailed in vitro pharmacological characterization of the clinically viable NOP receptor antagonist BTRX-246040

Federica Ferrari, Sabrina Rizzo, Chiara Ruzza, and Girolamo Calo'

FF, SR, CR, GC: Department of Medical Sciences, Section of Pharmacology, University of Ferrara, via Fossato di Mortara 19, 44121 Ferrara, Italy.

CR: Technopole of Ferrara, LTTA Laboratory for Advanced Therapies, Ferrara, Italy.

Running title: in vitro characterization of BTRX-246040

Corresponding author:

Chiara Ruzza, PhD

Department of Medical Sciences,

Section of Pharmacology,

via Fossato di Mortara 19, 44121 Ferrara, Italy.

chiara.ruzza@unife.it

Number of words in the Abstract: 183
Number of words in the Introduction: 590
Number of words in the Discussion: 1298

Nonstandard abbreviations: DMR, dynamic mass redistribution; mVD, mouse vas deferens; N/OFQ, nociceptin/orphanin FQ; NOP, N/OFQ peptide receptor

Abstract

The peptide nociceptin/orphanin FQ (N/OFQ) is the natural ligand of the N/OFQ receptor (NOP) which is widely expressed in the central and peripheral nervous system. Selective NOP antagonists are worthy of testing as innovative drugs to treat depression, Parkinson's disease, and drug abuse. The aim of this study was to perform a detailed in vitro characterization of BTRX-246040 (also known as LY2940094, [2-[4-[(2-chloro-4,4-difluoro-spiro[5H-thieno[2,3-c]pyran-7,4'-piperidine]-1'-yl)methyl]-3-methyl-pyrazol-1-yl]-3-pyridyl]methanol)a novel NOP antagonist that has been already studied in humans. BTRX-246040 has been tested in vitro in the following assays: calcium mobilization in cells expressing NOP and classical opioid receptors and chimeric G proteins, BRET assay measuring NOP interaction with G proteins and β-arrestins, the label free dynamic mass redistribution assay, and the electrically stimulated mouse vas deferens. BTRX-246040 was systematically compared to the standard NOP antagonist SB-612111. In all assays BTRX-246040 behaves as a pure and selective antagonist at human recombinant and murine native NOP receptors displaying 3 - 10 fold higher potency than the standard antagonist SB-612111. BTRX-246040 is as an essential pharmacological tool to further investigate the therapeutic potential of NOP antagonists in preclinical and clinical studies.

Significance Statement

NOP antagonists may be innovative antidepressant drugs. In this research the novel clinically viable NOP antagonist BTRX-246040 has been deeply characterized in vitro in a panel of assays. BTRX-246040 resulted a pure, potent and selective NOP antagonist.

JPET Fast Forward. Published on January 14, 2020 as DOI: 10.1124/jpet.119.262865
This article has not been copyedited and formatted. The final version may differ from this version.

Introduction

The peptide nociceptin/orphanin FQ (N/OFQ) is the natural ligand of the N/OFQ receptor (NOP) which is widely expressed in the central and peripheral nervous system (Lambert, 2008). Through the activation of the NOP receptor N/OFQ regulates different biological functions and pathological states (Lambert, 2008). NOP receptor agonists are now under clinical development for the treatment of hypertension (Kantola et al., 2017), urinary incontinence (Angelico et al., 2019) and pain (Calo and Lambert, 2018; Tzschentke et al., 2019). Several chemically diverse NOP antagonists have been described in the literature including the peptides [Nphe^{1}]N/OFQ(1-13)-NH_2 (Calo et al., 2000) and UFP-101 (Calo et al., 2002), and the small molecules J-113397 (Ozaki et al., 2000), SB-612111 (Zaratin et al., 2004), and Comp 24 (Goto et al., 2006) (for a review see (Toll et al., 2016; Zaveri and Meyer, 2019)). The crystal structure of the NOP receptor in complex with Comp 24 has been described (Thompson et al., 2012; Miller et al., 2015). The availability of selective antagonists together with mice (Nishi et al., 1997) and rats (Homberg et al., 2009; Rizzi et al., 2011) knockout for the NOP gene allowed researchers to study the consequences of blocking NOP signaling in animal models of pathology. A large series of studies suggest that selective NOP antagonists may represent innovative drugs to treat depression (Gavioli and Calo, 2013) and Parkinson's disease (Mercatelli et al., 2019). Moreover, recent findings suggest that treatment of drug abuse might be an additional indication for NOP antagonists (Rorick-Kehn et al., 2016; Kallupi et al., 2017) (see for a detailed discussion of this topic (Ciccocioppo et al., 2019)).

Recently a novel NOP receptor antagonist, BTRX-246040 (also known as LY2940094, [2-[4-[(2-chloro-4,4-difluoro-spiro[5H-thieno[2,3-c]pyran-7,4'-piperidine]-1'-yl)methyl]-3-methyl-pyrazol-1-yl]-3-pyridyl]methanol) has been discovered (Toledo et al., 2014). BTRX-246040 displays high affinity, functional potency and selectivity for the NOP receptor vs classical opioid proteins (Toledo et al., 2014; Statnick et al., 2016). In rodents BTRX-246040 produced robust antidepressant effects (Post et al., 2016b; Witkin et al., 2016), and displayed potential therapeutic utility in treating alcohol addiction (Rorick-Kehn et al., 2016) and disorders of appetitive behavior (Statnick et al., 2016). Moreover, in small proof of concept clinical studies BTRX-246040 was safe and well tolerated and showed efficacy in depressed (Post et al., 2016b) and alcohol dependent (Post et al., 2016a) patients (for an updated review on this NOP ligand see Witkin et al., 2019).

Despite increasing information regarding the in vivo actions of BTRX-246040 the pharmacological profile in vitro of this clinically viable NOP antagonist is very limited. Since a well-grounded

knowledge of the pharmacological profile of a receptor ligand is based on the analysis of its actions in different assays and preparations, the aim of this study was to carry out a detailed in vitro pharmacological characterization of BTRX-246040 using multiple assays including calcium mobilization in cells coexpressing NOP or classical opioid receptors and chimeric G proteins (Camarda et al., 2009; Camarda and Calo, 2013), bioluminescence resonance energy transfer (BRET) assay measuring NOP interaction with G proteins and β-arrestins (Malfacini et al., 2015), and the label free dynamic mass redistribution (DMR) assay (Malfacini et al., 2018). Moreover, in order to obtain information on the action of BTRX-246040 at native NOP receptors the last series of experiments were done in the electrically stimulated mouse vas deferens (mVD) (Calo et al., 1996). In all the above mentioned assays the effects of BTRX-246040 were compared to those of the standard NOP antagonist SB-612111 (Zaratin et al., 2004; Spagnolo et al., 2007).

Material and Methods

Drugs - N/OFQ, dermorphin, and dynorphin A were synthesized in house. DPDPE and naltrexone were from Tocris bioscience (Bristol, UK). SB-612111 and BTRX-246040 were provided by BlackThorn Therapeutics. 1 mM stock solution of N/OFQ, dermorphin, DPDPE, and dynorphin A were made in bidistilled water, while BTRX-246040, SB-612111, and naltrexone were solubilized in DMSO (10 mM). Stock solutions were kept at -20 °C until use.

Calcium mobilization assay - CHO cells expressing the human NOP, or kappa, or mu receptor and the C-terminally modified $G\alpha_{qi5}$ and CHO cells expressing the delta receptor and the $G\alpha_{qG66Di5}$ protein were generated and cultured as described previously (Camarda et al., 2009; Camarda and Calo, 2013). Cells were seeded at a density of 50,000 cells/well into 96-well black, clear-bottom plates 20 hours before the experiment. The day of the experiment, cells were loaded with 2.5 mM probenecid, 3 μM of the calcium sensitive fluorescent dye Fluo-4 AM and 0.01% pluronic acid in HBSS. After 30 min, the loading solution was removed and 100 μl/well of HBSS containing 20 mM HEPES, 2.5 mM probenecid and 500 μM Brilliant Black (Sigma Aldrich) were added. Serial dilutions were carried out in HBSS / HEPES (20 mM) buffer (containing 0.02% bovine serum albumin fraction V). The plate reader FlexStation II (Molecular Devices, Sunnyvale, CA) was used to measure fluorescence changes. On-line additions were carried out in a volume of 50 μl/well. All the experiments were performed at 37 °C. To facilitate drug diffusion into the wells, in antagonism experiments, three cycles of mixing (25 μl

from each well moved up and down 3 times) were performed immediately after antagonist injection. Antagonists were injected 24 min before agonists. Agonist effects were expressed as maximum change in percent over the baseline fluorescence. Baseline fluorescence was measured in wells treated with vehicle.

BRET assay - HEK293 cells co-expressing the different pairs of fusion proteins (NOP-RLuc / Gβ1-RGFP and NOP-RLuc / β-arrestin 2-RGFP) were generated and cultured as previously described (Malfacini et al., 2015). Enriched plasma membrane aliquots, used for G-protein experiments, were prepared from transfected cells as described by Vachon et al. (1987). The protein concentration in membrane preparations was determined with the QPRO-BCA kit (Cyanagen Srl, Bologna, IT) and Beckman DU 520 spectrophotometer (Brea, CA). Membrane experiments were performed in96-well untreated white opaque microplates, while whole cells experiments were performed in96-well sterile poly-D-lysine-coated white opaque microplates (PerkinElmer, Waltham, MA). The luminometer Victor 2030 (PerkinElmer, Waltham, MA) was used. For NOP/G-protein interaction evaluation, cell membranes (3 μg proteins / well) were suspended in DPBS. For the determination of NOP/β-arrestin 2 interaction, whole cells (100,000 cells/well) were seeded 24 h before the experiment. The day of the experiment, cell medium was removed and PBS containing $MgCl_2$ (0.5 mM) and $CaCl_2$ (0.9 mM) was added. Coelenterazine (5 μM) was injected 15 min prior reading the cell plate. Ligands were added 5 min before luminescence reading. In antagonism experiments, BTRX-246040 and SB-612111 were injected into the wells 15 min before N/OFQ and luminescence reading was started 60 min after N/OFQ injection. CPS measured for the RGFP and RLuc light emitted using 510(10) and 460(25)filters (PerkinElmer, Waltham, MA),respectively, were used to calculate BRET ratio. All data are expressed as stimulated BRET ratio, i.e. the ratio between CPS from RGFP and RLuc in the presence of ligands minus the BRET ratio in vehicle treated wells. Maximal agonist effects were expressed as fraction of the N/OFQ maximal effect, which was determined in each plate. All the experiments were performed at room temperature.

DMR assay – we would like to thank prof. D.G. Lambert (University of Leicester, UK) for kindly providing CHO cells stably expressing the human NOP. Cells were cultured as described by Malfacini and colleagues (Malfacini et al., 2018). The EnSight Multimode Plate Reader (Perkin Elmer, MA, US) was used for measuring DMR. 20 hours before the experiment, cells were seeded (15,000 cells/ well / 30 μl) into fibronectin-coated 384 well DMR microplates. Cells were starved in assay buffer (HBSS with 20 mM HEPES, 0.01% Bovine Serum Albumin (BSA) fraction V) for 90 min before the test.

JPET Fast Forward. Published on January 14, 2020 as DOI: 10.1124/jpet.119.262865
This article has not been copyedited and formatted. The final version may differ from this version.

Serial dilutions of ligands were made in the assay buffer. After reading baseline, compounds were added in a volume of 10 μL. Antagonists were incubated 30 min before N/OFQ injection, then DMR changes were recorded for 60 min. Responses were described as picometer (pm) shifts over time (sec) following subtraction of values from vehicle treated wells. Maximum picometers (pm) modification (Peak) was used to generate concentration response curves. All the experiments were carried out at 37°C.

Electrically stimulated mVD assay - All animal care and experimental procedures conformed to the European Communities Council directives (2010/63/EU) and national regulations (D.L. 26/2014). Studies involving animals are reported in accordance with the ARRIVE guidelines (Kilkenny et al., 2010). This study was approved by the Italian Ministry of Health (authorization number 302/2017-PR). The experiments were performed on the mouse vas deferens. The tissues were taken from male, specific pathogen free, CD-1 mice (40 g, Laboratory for Preclinical Research (LARP) of the University of Ferrara, Italy). Mice were housed under standard conditions (22°C, 55% humidity, 12 h light/dark cycle, light on at 7:00 am), with free access to food and water. Appropriate environmental enrichment was present in each cage. Mice were killed with CO_2 overdose. Bioassay experiments were performed as previously described (Calo et al., 1996). The electrically evoked contractions were measured by means of Basile strain gauge isotonic transducers (Basile 7006, Ugo Basile srl, Varese, Italy) and recorder with the Power Lab 8 system ((ADInstruments, Colorado Springs). After 60 min equilibration , the contractions induced by electrical field stimulation were stable. At this time, cumulative concentration response curve to agonists were performed (0.5 log unit steps). Antagonists were added 15 min before agonists. Data are expressed as % of the control twitch. The injection of vehicle did not modify the electrically induced twitch. A total number of 10 mice has been used for this study.

Data analysis and terminology - The pharmacological terminology adopted in this paper is consistent with IUPHAR recommendations (Neubig et al., 2003). All data are expressed as the mean ± standard error of the mean (SEM) of at least 3 experiments. For potency values 95% confidence limits ($CL_{95\%}$) were indicated. Agonist potencies are given as pEC_{50} that is the negative logarithm to base 10 of the molar concentration of an agonist that produces 50% of the maximal effect of that agonist. Concentration-response curves to agonists were fitted to the classical four-parameter logistic nonlinear regression model: $Effect=Baseline+(E_{max}-Baseline)/(1+10^{(LogEC_{50}-Log[compound])*Hillslope})$. Curves fitting were performed using PRISM 6.0 (GraphPad Software In., San Diego). SB-612111 was assayed at single concentrations against the concentration-response curve to N/OFQ and its potency expressed as

JPET Fast Forward. Published on January 14, 2020 as DOI: 10.1124/jpet.119.262865
This article has not been copyedited and formatted. The final version may differ from this version.

pA_2 derived from the following equation: pA_2=-log[(CR−1)/[A]], assuming a slope value equal to unity, where CR indicates the ratio between agonist potency in the presence and absence of antagonist and [A] is the molar concentration of the antagonist (Kenakin, 2004). BTRX-246040 was tested using the classical Schild protocol. Antagonist potencies were expressed either as pA_2 or pK_B depending on the type of antagonism. For competitive type of antagonism, pA_2 values were derived from the classical Schild protocol. For non-competitive type of antagonism, pK_B values were obtained by the Gaddum method (Gaddum et al., 1955). In practice, equiactive concentrations of the agonist in the absence ([A]) and presence ([A']) of a noncompetitive antagonist ([B]) are compared in a double reciprocal plot describing a straight line, and pK_B was derived from the equation: pK_B = log [(slope – 1)/[B]]. Data have been statistically analyzed using one-way ANOVA followed by the Dunnett's post hoc test. $P < 0.05$ was considered statistically significant.

Results

CHO $_{NOP + G\alpha qi5}$ cells N/OFQ increased calcium levels in a concentration dependent manner showing high potency (pEC_{50} value of 9.65 (9.03 – 9.98)) and maximal effects (E_{max} 353±15%), while SB-612111 and BTRX-246040 were inactive up to 10 µM (Fig 1, panel A). SB-612111, 100 nM, shifted to right the concentration response curve to N/OFQ without changing the agonist maximal effect. A pA_2 value of 8.86 ($CL_{95\%}$ 8.31 – 9.41) was calculated from these experiments (Fig 1, panel B). BTRX-246040, in the range of concentrations 1-1000 nM, elicited a concentration dependent dextral displacement of the concentration response curve to N/OFQ, with a slight depression of maximal effects at the higher concentrations tested (Fig 1, panel C). A pA_2 value of 9.27 ($CL_{95\%}$ 8.85 – 9.69) was extrapolated from the Schild plot (Fig 1, panel D). In CHO cells expressing chimeric G proteins and classical opioid receptors, standard agonists (dermorphin for mu, DPDPE for delta, and dynorphin A for kappa receptors) elicited concentration dependent stimulatory effects, that were competitively antagonized by naltrexone with pA_2 values of 8.55 ($CL_{95\%}$ 8.07 – 9.03), 7.42 ($CL_{95\%}$ 7.17 – 7.67), and 8.53 ($CL_{95\%}$ 7.78 – 9.28), respectively (Fig 2). At 1 µM, SB-612111 was inactive at mu and delta receptors but behaved as a low potency antagonist at the kappa receptor (pA_2 6.14, 5.69 – 6.59). 1 µM BTRX-246040 was inactive at delta and kappa receptors, while producing a small but consistent shift of the concentration response curve to dermorphin (pA_2 6.60, 6.34 – 6.85) (Fig 3).

In membranes prepared from HEK293 cells stably coexpressing the NOP/RLuc and Gβ1/RGFP fusoproteins, N/OFQ promoted receptor/G protein interaction in a concentration dependent manner,

showing high potency (pEC_{50} 8.94 (8.73 – 9.15)) and maximal effects. In parallel experiments, SB-612111 was inactive while BTRX-246040 elicited a very small reduction of the BRET ratio in a concentration dependent manner (Fig 4, panel A). SB-612111, 10 nM, produced a rightward shift of the concentration response curve to N/OFQ with no changes of the E_{max}. A pA_2 value of 8.96 ($CL_{95\%}$ 8.05 – 9.87) was calculated from these experiments (Fig 4, panel C). BTRX-246040, in the range of concentrations 1-1000 nM, elicited a concentration dependent dextral displacement of the concentration response curve to N/OFQ with a significant reduction of N/OFQ E_{max} (Fig 4, panel E). A pK_B value of 9.53 (8.65 – 10.41) was calculated for BTRX-246040 from these experiments. In HEK293 cells stably coexpressing the NOP/RLuc and the β-arrestin 2/RGFP fusoproteins, N/OFQ promoted receptor/β-arrestin 2 interaction in a concentration dependent manner with high potency (pEC_{50} value of 8.23 (8.16 – 8.30)) and maximal effects, while SB-612111 and BTRX-246040 were inactive up to micromolar concentrations (Fig 4, panel B). SB-612111, 10 nM, produced a dextral displacement of the concentration response curve to N/OFQ without modifying agonist maximal effect, with a pA_2 of 8.70 ($CL_{95\%}$ 7.91 – 9.49) (Fig 4, panel D). BTRX-246040, 1-1000 nM, elicited a concentration dependent rightward shift of the concentration response curve to N/OFQ, with a large depression of maximal effects (Fig 4, panel F). A pK_B value of 9.16 (8.00 – 10.32) was calculated from these experiments.

In CHO_{NOP} cells, N/OFQ elicited a concentration dependent positive DMR response while SB-612111 was inactive up to micromolar concentrations. BTRX-246040 elicited a very small negative DMR response in a concentration dependent manner (Fig 5 panel A). In the presence of 100 nM SB-612111, the curve to N/OFQ was rightward shifted with no changes of the agonist maximal effects. A pA_2 value of 8.21 ($CL_{95\%}$ 7.32 – 8.75) was derived for SB-612111 from these experiments (Fig 5 panel B). BTRX-246040, in the 10 - 1000 nM range, promoted a concentration dependent dextral displacement of the concentration response curve to N/OFQ, associated with a small reduction of maximal effects (Fig 5 panel C). The Schild analysis of these data yielded a pA_2 of 8.88 ($CL_{95\%}$ 8.63 – 9.13) (Fig 5, panel D).

In the isolated mouse vas deferens, N/OFQ inhibited the electrically induced twitch in a concentration dependent manner with a pEC_{50} of 7.45 (7.28 – 7.62), while SB-612111 and BTRX-246040 were inactive up to 1 μM. At 100 nM, SB-612111 elicited a rightward shift of the curve to N/OFQ, displaying a pA_2 value of 7.89 ($CL_{95\%}$ 7.59 – 8.19) (Fig 6, panel A). BTRX-246040, in the 10 - 1000 nM, range elicited a concentration dependent dextral displacement of the concentration response curve to N/OFQ, without changing its E_{max} (Fig. 6, panel B). The Schild analysis of this set of data was

compatible with a competitive type of interaction and yielded a pA_2 value of 8.45 ($CL_{95\%}$ 7.91 - 8.99) (Fig. 6, panel C). Finally, under the same experimental conditions, 1 μM BTRX-246040 did not modify the inhibitory effects elicited by the delta agonist DPDPE (Fig. 6, panel D).

The results obtained in this study, together with data from literature, have been summarized in Table 1.

Discussion

The present study extends previous findings (Toledo et al., 2014; Statnick et al., 2016) demonstrating that BTRX-246040 behaves as a pure and selective antagonist at human recombinant and murine native NOP receptors displaying 3-10 fold higher potency than the standard antagonist SB-612111.

BTRX-246040 behaved as a pure NOP antagonist; this is demonstrated by the lack of effect per se in the calcium mobilization and bioassay studies as well as in previous GTPγS binding experiments (Statnick et al., 2016). In NOP/G protein BRET and in DMR experiments, BTRX-246040 elicited very small effects opposite to those of N/OFQ, thus suggesting an inverse agonist behavior of this NOP ligand. However, the putative effects of BTRX-246040 were too small to be further investigated. It should be mentioned in this regard that the NOP receptor has very low liability to display constitutive activity. This has been clearly demonstrated in previous receptor/G protein BRET studies where, under the same experimental conditions, GDP inhibited in a concentration dependent manner mu and particularly delta opioid receptor interaction with G protein (Vezzi et al., 2013) while producing negligible effects on NOP/G protein interaction (Malfacini et al., 2015). Thus, to investigate the possible inverse agonist activity of BTRX-246040 further studies employing constitutively active mutants of the NOP receptor e.g. NOP_{N133W} (Kam et al., 2002) or overexpression of NOP receptors via microinjection of cDNA plasmids (Mahmoud et al., 2010) are needed.

As far as type of antagonism is concerned, contrasting results were obtained in the various assays. In fact, although a typical competitive interaction for BTRX-246040 and N/OFQ has been measured in the mouse vas deferens bioassay, a small but statistically significant depression of N/OFQ maximal effects has been induced by high concentrations of BTRX-246040 in calcium mobilization and DMR experiments, while a more profound reduction of agonist maximal effects was measured in BRET studies. These variable results deserve attention. For calcium mobilization experiments, it is well known that the rapid and transient nature of calcium peaks causes hemi equilibrium conditions and this may lead to an apparent unsurmountable behavior of competitive antagonists (Charlton and Vauquelin,

JPET Fast Forward. Published on January 14, 2020 as DOI: 10.1124/jpet.119.262865
This article has not been copyedited and formatted. The final version may differ from this version.

2010). In calcium mobilization studies, the NOP competitive antagonist C-24 generated results very similar to those reported here with BTRX-246040 (Fischetti et al., 2009). In previous NOP/G protein BRET studies it has been reported that after 5 min of incubation with N/OFQ the antagonists UFP-101 and J-113397 displayed a surmountable type of antagonism while C-24 and SB-612111 caused a significant depression of N/OFQ maximal effects; this depression was no longer evident by prolonging the incubation time with N/OFQ to 15 min (Malfacini et al., 2015). Under these experimental conditions (15 min incubation time with the agonist), BTRX-246040 displayed an unsurmountable type of antagonism (data not shown). Based on the previous findings obtained with SB-612111 we further prolonged incubation time to 30 and 60 min. However, even though the depression of N/OFQ E_{max} was smaller with longer incubation times, a depression of N/OFQ maximal effects was still clearly evident after one hour of incubation.. Since multi-flexible docking studies (Della Longa and Arcovito, 2018) clearly demonstrated that BTRX-246040 binds the NOP receptor in the same binding pocket recognizing competitive antagonists such as C-24 (Thompson et al., 2012) and SB-612111 (Miller et al., 2015), it is reasonable to suggest that the BTRX-246040 unsurmountable behavior derives from a very slow rate of offset that does not allow equilibrium to be reached even with prolonged incubation times (Kenakin, 2004). The involvement of kinetic factors in the unsurmountable behavior of BTRX-246040 is also suggested by the fact that the maximal effects of N/OFQ were more depressed measuring receptor / β-arrestin 2 than receptor / G protein interaction. This may be due to the fact that the kinetics of receptor / G protein interaction is much faster (half time in the range 6 – 12 sec) than that of receptor / β-arrestin 2 interaction (half time in the range 60 – 130 s) (Molinari et al., 2010). The above considerations may also explain the unsurmountable behavior displayed by BTRX-246040 in DMR experiments however they go against the typical competitive interaction displayed by the antagonist in the electrically stimulated mouse vas deferens assay. Although a large series of studies demonstrated that the murine NOP receptor displays a pharmacological profile very similar if not identical to that of the human NOP receptor (see table 1 in (Malfacini and Calo, 2019)), it is still possible that subtle species specific receptor differences may explain the different behavior of BTRX-246040.

As far as antagonist potency is concerned, BTRX-246040 displayed very high and consistent potency (range 8.45 – 9.58) in the various assays; these results are in line with the potency (9.77) previously reported in stimulated GTPγS binding studies as well as with the affinity (9.98) obtained in receptor binding experiments (Statnick et al., 2016). Importantly, compared to the standard NOP antagonist SB-

JPET Fast Forward. Published on January 14, 2020 as DOI: 10.1124/jpet.119.262865
This article has not been copyedited and formatted. The final version may differ from this version.

612111 in parallel experiments, BTRX-246040 was always found to be 3 to 10 fold more potent. Of note the values of SB-612111 potency obtained in the present study in the different assays were very close to those previously reported in the literature (Spagnolo et al., 2007; Malfacini et al., 2015; Ferrari et al., 2017; Malfacini et al., 2018). Therefore, based on the present and previous findings (reviewed in (Toll et al., 2016; Malfacini and Calo, 2019)) we may propose the following rank order of potency of antagonists BTRX-246040 > SB-612111 > J-113397 > UFP-101 as a NOP pharmacological fingerprint. Moreover, a strong correlation between NOP antagonist potency and receptor thermostability has been previously demonstrated that is consistent with a reduction in receptor flexibility by shifting the conformational equilibrium exclusively to the receptor inactive state (Miller et al., 2015). On this basis, it is reasonable to suggest that BTRX-246040 is an ideal candidate for further NOP crystallization studies.

Together with potency, selectivity of action is another key feature of a receptor antagonist. In calcium mobilization studies BTRX-246040 was approximately 1000 fold selective for NOP over classical opioid receptors and in bioassay studies the estimated NOP selectivity of BTRX-246040 over delta receptor was > 300. These results are perfectly in line with published receptor binding data (Statnick et al., 2016) that demonstrated that BTRX-246040 affinity is > 3000 fold higher for NOP than opioid receptors. In parallel experiments SB-612111 displayed high NOP selectivity confirming previous findings (Zaratin et al., 2004; Spagnolo et al., 2007). Thus, collectively these findings suggest that BTRX-246040 is more potent and as NOP selective as SB-612111. The high NOP selectivity of BTRX-246040 demonstrated in vitro is corroborated by in vivo findings: in fact, the antidepressant (Witkin et al., 2016) and anorectic (Statnick et al., 2016) actions of BTRX-246040 were no longer evident in mice knockout for the NOP receptor gene.

In conclusion, the results of the present study demonstrated that BTRX-246040 is pure, potent and selective antagonist of the NOP receptor. Compared with the standard NOP antagonist SB-612111, BTRX-246040 displays similar high NOP selectivity being however 3-10 fold more potent. These pharmacodynamic features are associated with great pharmacokinetic properties demonstrated in rodents and humans (Raddad et al., 2016). In addition, the tolerability and safety of BTRX-246040 once-daily dosing of 40 mg up to 8 weeks have been already demonstrated in clinical studies (Witkin et al., 2019). Collectively these features candidate BTRX-246040 as an essential pharmacological tool to further investigate the therapeutic potential of NOP antagonists as innovative drugs to treat depression (Gavioli and Calo, 2013), Parkinson's disease (Mercatelli et al., 2019), and possibly drug abuse

(Ciccocioppo et al., 2019) as well as to identify novel conditions/diseases where the blockade of the NOP receptor is associated with beneficial effects, including traumatic injuries of the central nervous system (Awwad et al., 2018; Sekine et al., 2018), post-traumatic stress disorders (Zhang et al., 2015; Genovese and Dobre, 2017), and sepsis (Carvalho et al., 2008; Williams et al., 2008).

Acknowledgements

We thank BlackThorn Therapeutics (San Francisco, CA, USA) for providing BTRX-246040 and SB-612111.

Authorship Contributions

Participated in research design: Ferrari, Ruzza, and Calò.

Conducted experiments: Ferrari and Rizzo

Performed data analysis: Ferrari, Rizzo, and Ruzza

Wrote the manuscript: Ruzza and Calò

References

Angelico P, Barchielli M, Lazzeri M, Guerrini R and Calo G (2019) Nociceptin/Orphanin FQ and Urinary Bladder. Handbook of experimental pharmacology 254:347-365.

Awwad HO, Durand CD, Gonzalez LP, Tompkins P, Zhang Y, Lerner MR, Brackett DJ, Sherry DM, Awasthi V and Standifer KM (2018) Post-blast treatment with Nociceptin/Orphanin FQ peptide (NOP) receptor antagonist reduces brain injury-induced hypoxia and signaling proteins in vestibulomotor-related brain regions. Behavioural brain research 340:183-194.

Calo G, Guerrini R, Bigoni R, Rizzi A, Marzola G, Okawa H, Bianchi C, Lambert DG, Salvadori S and Regoli D (2000) Characterization of [Nphe(1)]nociceptin(1-13)NH(2), a new selective nociceptin receptor antagonist. British journal of pharmacology 129:1183-1193.

Calo G and Lambert DG (2018) Nociceptin/orphanin FQ receptor ligands and translational challenges: focus on cebranopadol as an innovative analgesic. British journal of anaesthesia 121:1105-1114.

Calo G, Rizzi A, Bogoni G, Neugebauer V, Salvadori S, Guerrini R, Bianchi C and Regoli D (1996) The mouse vas deferens: a pharmacological preparation sensitive to nociceptin. European journal of pharmacology 311:R3-5.

Calo G, Rizzi A, Rizzi D, Bigoni R, Guerrini R, Marzola G, Marti M, McDonald J, Morari M, Lambert DG, Salvadori S and Regoli D (2002) [Nphe1,Arg14,Lys15]nociceptin-NH2, a novel potent and selective antagonist of the nociceptin/orphanin FQ receptor. British journal of pharmacology 136:303-311.

Camarda V and Calo G (2013) Chimeric G proteins in fluorimetric calcium assays: experience with opioid receptors. Methods in molecular biology 937:293-306.

Camarda V, Fischetti C, Anzellotti N, Molinari P, Ambrosio C, Kostenis E, Regoli D, Trapella C, Guerrini R, Severo S and Calo G (2009) Pharmacological profile of NOP receptors coupled with calcium signaling via the chimeric protein G alpha qi5. Naunyn-Schmiedeberg's archives of pharmacology 379:599-607.

Carvalho D, Petronilho F, Vuolo F, Machado RA, Constantino L, Guerrini R, Calo G, Gavioli EC, Streck EL and Dal-Pizzol F (2008) The nociceptin/orphanin FQ-NOP receptor antagonist effects on an animal model of sepsis. Intensive care medicine 34:2284-2290.

Charlton SJ and Vauquelin G (2010) Elusive equilibrium: the challenge of interpreting receptor pharmacology using calcium assays. British journal of pharmacology 161:1250-1265.

Ciccocioppo R, Borruto AM, Domi A, Teshima K, Cannella N and Weiss F (2019) NOP-Related Mechanisms in Substance Use Disorders. Handbook of experimental pharmacology 254:187-212.

Della Longa S and Arcovito A (2018) "In silico" study of the binding of two novel antagonists to the nociceptin receptor. Journal of computer-aided molecular design 32:385-400.

Ferrari F, Malfacini D, Journigan BV, Bird MF, Trapella C, Guerrini R, Lambert DG, Calo G and Zaveri NT (2017) In vitro pharmacological characterization of a novel unbiased NOP receptor-selective nonpeptide agonist AT-403. Pharmacology research & perspectives 5.

Fischetti C, Camarda V, Rizzi A, Pela M, Trapella C, Guerrini R, McDonald J, Lambert DG, Salvadori S, Regoli D and Calo G (2009) Pharmacological characterization of the nociceptin/orphanin FQ receptor non peptide antagonist Compound 24. European journal of pharmacology 614:50-57.

Gaddum JH, Hameed KA, Hathway DE and Stephens FF (1955) Quantitative studies of antagonists for 5-hydroxytryptamine. Quarterly journal of experimental physiology and cognate medical sciences 40:49-74.

Gavioli EC and Calo G (2013) Nociceptin/orphanin FQ receptor antagonists as innovative antidepressant drugs. Pharmacology & therapeutics 140:10-25.

Genovese RF and Dobre S (2017) Mitigation of adverse behavioral impact from predator exposure by the nociceptin/orphanin FQ peptide antagonist J-113397 in rats. Behavioural pharmacology 28:521-530.

Goto Y, Arai-Otsuki S, Tachibana Y, Ichikawa D, Ozaki S, Takahashi H, Iwasawa Y, Okamoto O, Okuda S, Ohta H and Sagara T (2006) Identification of a novel spiropiperidine opioid receptor-like 1 antagonist class by a focused library approach featuring 3D-pharmacophore similarity. Journal of medicinal chemistry 49:847-849.

Homberg JR, Mul JD, de Wit E and Cuppen E (2009) Complete knockout of the nociceptin/orphanin FQ receptor in the rat does not induce compensatory changes in mu, delta and kappa opioid receptors. Neuroscience 163:308-315.

Kallupi M, Scuppa G, de Guglielmo G, Calo G, Weiss F, Statnick MA, Rorick-Kehn LM and Ciccocioppo R (2017) Genetic Deletion of the Nociceptin/Orphanin FQ Receptor in the Rat Confers Resilience to the Development of Drug Addiction. Neuropsychopharmacology : official publication of the American College of Neuropsychopharmacology 42:695-706.

Kam KW, New DC and Wong YH (2002) Constitutive activation of the opioid receptor-like (ORL1) receptor by mutation of Asn133 to tryptophan in the third transmembrane region. Journal of neurochemistry 83:1461-1470.

Kantola I, Scheinin M, Gulbrandsen T, Meland N and Smerud KT (2017) Safety, Tolerability, and Antihypertensive Effect of SER100, an Opiate Receptor-Like 1 (ORL-1) Partial Agonist, in Patients With Isolated Systolic Hypertension. Clinical pharmacology in drug development 6:584-591.

Kenakin T (2004) A Pharmacology Primer. Elsevier Academic Press, San Diego.

Kilkenny C, Browne WJ, Cuthill IC, Emerson M and Altman DG (2010) Improving bioscience research reporting: the ARRIVE guidelines for reporting animal research. PLoS biology 8:e1000412.

Lambert DG (2008) The nociceptin/orphanin FQ receptor: a target with broad therapeutic potential. Nature reviews Drug discovery 7:694-710.

Mahmoud S, Margas W, Trapella C, Calo G and Ruiz-Velasco V (2010) Modulation of silent and constitutively active nociceptin/orphanin FQ receptors by potent receptor antagonists and Na+ ions in rat sympathetic neurons. Molecular pharmacology 77:804-817.

Malfacini D, Ambrosio C, Gro MC, Sbraccia M, Trapella C, Guerrini R, Bonora M, Pinton P, Costa T and Calo G (2015) Pharmacological Profile of Nociceptin/Orphanin FQ Receptors Interacting with G-Proteins and beta-Arrestins 2. PloS one 10:e0132865.

Malfacini D and Calo G (2019) Pharmacological Assays for Investigating the NOP Receptor. Handbook of experimental pharmacology 254:69-89.

Malfacini D, Simon K, Trapella C, Guerrini R, Zaveri NT, Kostenis E and Calo G (2018) NOP receptor pharmacological profile - A dynamic mass redistribution study. PloS one 13:e0203021.

Mercatelli D, Pisano CA, Novello S and Morari M (2019) NOP Receptor Ligands and Parkinson's Disease. Handbook of experimental pharmacology 254:213-232.

Miller RL, Thompson AA, Trapella C, Guerrini R, Malfacini D, Patel N, Han GW, Cherezov V, Calo G, Katritch V and Stevens RC (2015) The Importance of Ligand-Receptor Conformational Pairs in Stabilization: Spotlight on the N/OFQ G Protein-Coupled Receptor. Structure 23:2291-2299.

Molinari P, Vezzi V, Sbraccia M, Gro C, Riitano D, Ambrosio C, Casella I and Costa T (2010) Morphine-like opiates selectively antagonize receptor-arrestin interactions. The Journal of biological chemistry 285:12522-12535.

Neubig RR, Spedding M, Kenakin T, Christopoulos A, International Union of Pharmacology Committee on Receptor N and Drug C (2003) International Union of Pharmacology Committee on Receptor Nomenclature and Drug Classification. XXXVIII. Update on terms and symbols in quantitative pharmacology. Pharmacological reviews 55:597-606.

Nishi M, Houtani T, Noda Y, Mamiya T, Sato K, Doi T, Kuno J, Takeshima H, Nukada T, Nabeshima T, Yamashita T, Noda T and Sugimoto T (1997) Unrestrained nociceptive response and disregulation of hearing ability in mice lacking the nociceptin/orphaninFQ receptor. The EMBO journal 16:1858-1864.

Ozaki S, Kawamoto H, Itoh Y, Miyaji M, Azuma T, Ichikawa D, Nambu H, Iguchi T, Iwasawa Y and Ohta H (2000) In vitro and in vivo pharmacological characterization of J-113397, a potent and selective non-peptidyl ORL1 receptor antagonist. European journal of pharmacology 402:45-53.

Post A, Smart TS, Jackson K, Mann J, Mohs R, Rorick-Kehn L, Statnick M, Anton R, O'Malley SS and Wong CJ (2016a) Proof-of-Concept Study to Assess the Nociceptin Receptor Antagonist

LY2940094 as a New Treatment for Alcohol Dependence. Alcoholism, clinical and experimental research 40:1935-1944.

Post A, Smart TS, Krikke-Workel J, Dawson GR, Harmer CJ, Browning M, Jackson K, Kakar R, Mohs R, Statnick M, Wafford K, McCarthy A, Barth V and Witkin JM (2016b) A Selective Nociceptin Receptor Antagonist to Treat Depression: Evidence from Preclinical and Clinical Studies. Neuropsychopharmacology : official publication of the American College of Neuropsychopharmacology 41:1803-1812.

Raddad E, Chappell A, Meyer J, Wilson A, Ruegg CE, Tauscher J, Statnick MA, Barth V, Zhang X and Verfaille SJ (2016) Occupancy of Nociceptin/Orphanin FQ Peptide Receptors by the Antagonist LY2940094 in Rats and Healthy Human Subjects. Drug metabolism and disposition: the biological fate of chemicals 44:1536-1542.

Rizzi A, Molinari S, Marti M, Marzola G and Calo G (2011) Nociceptin/orphanin FQ receptor knockout rats: in vitro and in vivo studies. Neuropharmacology 60:572-579.

Rorick-Kehn LM, Ciccocioppo R, Wong CJ, Witkin JM, Martinez-Grau MA, Stopponi S, Adams BL, Katner JS, Perry KW, Toledo MA, Diaz N, Lafuente C, Jimenez A, Benito A, Pedregal C, Weiss F and Statnick MA (2016) A Novel, Orally Bioavailable Nociceptin Receptor Antagonist, LY2940094, Reduces Ethanol Self-Administration and Ethanol Seeking in Animal Models. Alcoholism, clinical and experimental research 40:945-954.

Sekine Y, Siegel CS, Sekine-Konno T, Cafferty WBJ and Strittmatter SM (2018) The nociceptin receptor inhibits axonal regeneration and recovery from spinal cord injury. Science signaling 11.

Spagnolo B, Carra G, Fantin M, Fischetti C, Hebbes C, McDonald J, Barnes TA, Rizzi A, Trapella C, Fanton G, Morari M, Lambert DG, Regoli D and Calo G (2007) Pharmacological characterization of the nociceptin/orphanin FQ receptor antagonist SB-612111 [(-)-cis-1-methyl-7-[[4-(2,6-dichlorophenyl)piperidin-1-yl]methyl]-6,7,8,9-tetrah ydro-5H-benzocyclohepten-5-ol]: in vitro studies. The Journal of pharmacology and experimental therapeutics 321:961-967.

Statnick MA, Chen Y, Ansonoff M, Witkin JM, Rorick-Kehn L, Suter TM, Song M, Hu C, Lafuente C, Jimenez A, Benito A, Diaz N, Martinez-Grau MA, Toledo MA and Pintar JE (2016) A Novel Nociceptin Receptor Antagonist LY2940094 Inhibits Excessive Feeding Behavior in Rodents: A Possible Mechanism for the Treatment of Binge Eating Disorder. The Journal of pharmacology and experimental therapeutics 356:493-502.

Thompson AA, Liu W, Chun E, Katritch V, Wu H, Vardy E, Huang XP, Trapella C, Guerrini R, Calo G, Roth BL, Cherezov V and Stevens RC (2012) Structure of the nociceptin/orphanin FQ receptor in complex with a peptide mimetic. Nature 485:395-399.

Toledo MA, Pedregal C, Lafuente C, Diaz N, Martinez-Grau MA, Jimenez A, Benito A, Torrado A, Mateos C, Joshi EM, Kahl SD, Rash KS, Mudra DR, Barth VN, Shaw DB, McKinzie D, Witkin JM and Statnick MA (2014) Discovery of a novel series of orally active nociceptin/orphanin FQ (NOP) receptor antagonists based on a dihydrospiro(piperidine-4,7'-thieno[2,3-c]pyran) scaffold. Journal of medicinal chemistry 57:3418-3429.

Toll L, Bruchas MR, Calo G, Cox BM and Zaveri NT (2016) Nociceptin/Orphanin FQ Receptor Structure, Signaling, Ligands, Functions, and Interactions with Opioid Systems. Pharmacological reviews 68:419-457.

Tzschentke TM, Linz K, Koch T and Christoph T (2019) Cebranopadol: A Novel First-in-Class Potent Analgesic Acting via NOP and Opioid Receptors. Handbook of experimental pharmacology 254:367-398.

Vachon L, Costa T and Herz A (1987) Opioid receptor desensitization in NG 108-15 cells. Differential effects of a full and a partial agonist on the opioid-dependent GTPase. Biochemical pharmacology 36:2889-2897.

Vezzi V, Onaran HO, Molinari P, Guerrini R, Balboni G, Calo G and Costa T (2013) Ligands raise the constraint that limits constitutive activation in G protein-coupled opioid receptors. The Journal of biological chemistry 288:23964-23978.

Williams JP, Thompson JP, Young SP, Gold SJ, McDonald J, Rowbotham DJ and Lambert DG (2008) Nociceptin and urotensin-II concentrations in critically ill patients with sepsis. British journal of anaesthesia 100:810-814.

Witkin JM, Rorick-Kehn LM, Benvenga MJ, Adams BL, Gleason SD, Knitowski KM, Li X, Chaney S, Falcone JF, Smith JW, Foss J, Lloyd K, Catlow JT, McKinzie DL, Svensson KA, Barth VN, Toledo MA, Diaz N, Lafuente C, Jimenez A, Benito A, Pedregal C, Martinez-Grau MA, Post A, Ansonoff MA, Pintar JE and Statnick MA (2016) Preclinical findings predicting efficacy and side-effect profile of LY2940094, an antagonist of nociceptin receptors. Pharmacology research & perspectives 4:e00275.

Witkin JM, Wallace TL, Martin WJ (2019) Therapeutic Approaches for NOP Receptor Antagonists in Neurobehavioral Disorders: Clinical Studies in Major Depressive Disorder and Alcohol Use Disorder with BTRX-246040 (LY2940094). Handb Exp Pharmacol. 254:399-415.

Zaratin PF, Petrone G, Sbacchi M, Garnier M, Fossati C, Petrillo P, Ronzoni S, Giardina GA and Scheideler MA (2004) Modification of nociception and morphine tolerance by the selective opiate receptor-like orphan receptor antagonist (-)-cis-1-methyl-7-[[4-(2,6-dichlorophenyl)piperidin-1-yl]methyl]-6,7,8,9-tetrahy dro-5H-benzocyclohepten-5-ol (SB-612111). The Journal of pharmacology and experimental therapeutics 308:454-461.

Zaveri NT and Meyer ME (2019) NOP-Targeted Nonpeptide Ligands. Handbook of experimental pharmacology 254:37-67.

Zhang Y, Simpson-Durand CD and Standifer KM (2015) Nociceptin/orphanin FQ peptide receptor antagonist JTC-801 reverses pain and anxiety symptoms in a rat model of post-traumatic stress disorder. British journal of pharmacology 172:571-582.

Footnotes

Financial support

This work has been financially supported by funds from the University of Ferrara [FAR grant to G.C.] and the Italian Ministry of Research [PRIN2015WX8Y5B grant to G.C.].

Figure legends

Figure 1. *Calcium mobilization assay*. Concentration-response curves to N/OFQ, SB-612111, and BTRX-246040 are displayed in panel A. Concentration-response curves to N/OFQ in the absence and presence of SB-612111 100 nM and BTRX-246040 1 nM– 1000 nM are shown in panels B and C respectively. The corresponding Schild plot is shown in panel D. Data are mean ± sem of 3 (panel A) or 4 (panels B – D) separate experiments performed in duplicate. * $p < 0.05$ vs control, according to one-way ANOVA followed by the Dunnett post hoc test.

Figure 2. Calcium mobilization assay in CHO cells coexpressing the mu (left panels), delta (middle panels), and kappa (right panels) receptors and chimeric G proteins. Concentration-response curves to dermorphin (panel A), DPDPE (panel B), and dynorphin A (panel C) in absence and presence of increasing concentrations (0.01 µM– 1 µM) of naltrexone. The corresponding Schild plots are shown in panels D, E, and F. Data are mean ± sem of 5 separate experiments performed in duplicate. * $p < 0.05$ vs control, according to one-way ANOVA followed by the Dunnett post hoc test.

Figure 3. Calcium mobilization assay in CHO cells coexpressing the mu (left panels), delta (middle panels), and kappa (right panels) receptors and chimeric G proteins. Concentration-response curves to dermorphin, DPDPE, and dynorphin A in absence and presence of SB-612111 1 µM (Panels A, B and C, respectively) and BTRX-246040 1 µM (Panels D, E and F, respectively). Data are mean ± sem of 5 separate experiments performed in duplicate.

Figure 4. *BRET assay*. NOP/G-protein (left panels) and NOP/β-arrestin 2 interaction (right panels) experiments. Concentration-response curves to N/OFQ, SB-612111, and BTRX-246040 are displayed in panels A and B. Concentration-response curves to N/OFQ in the absence and presence of SB-612111 10 nM (panels C and D) and BTRX-246040 1 nM– 1000 nM (panels E and F). Data are mean ± sem of 5 separate experiments performed in duplicate. * $p < 0.05$ vs control, according to one-way ANOVA followed by the Dunnett post hoc test.

Figure 5. *DMR assay*. Concentration-response curves to N/OFQ, SB-612111, and BTRX-246040 are displayed in panel A. Concentration-response curves to N/OFQ in the absence and presence of SB-612111 100 nM and BTRX-246040 10 nM– 1000 nM are shown in panels B and C respectively. The corresponding Schild plot is shown in panel D. Data are mean ± sem of 4 separate experiments

performed in duplicate. * $p < 0.05$ vs control, according to one-way ANOVA followed by the Dunnett post hoc test.

Figure 6. *mVD assay*. Concentration-response curves to N/OFQ in the absence and presence of SB-612111 100 nM (panel A) and of BTRX-246040 10 nM– 1000 nM (panel B). The corresponding Schild plot is shown in panel C. Panel D shows the concentration-response curves to DPDPE in absence and presence of BTRX-246040 1000 nM. Data are mean ± sem of 5 separate experiments performed in duplicate.

Table 1. Comparison of the NOP affinity and antagonistic potency of BTRX-246040 and SB-612111.

	BTRX-246040	SB-612111
Receptor binding	9.98	9.18
Stimulated GTPγS binding	9.77	9.70
Calcium mobilization	9.27	8.86
BRET G protein	9.53	8.96
BRET / β-arrestin 2	9.16	8.70
DMR	8.88	8.21
Mouse vas deferens	8.45	7.89

Receptor binding and stimulated GTPγS binding data are taken from Statnick et al., 2016 for BTRX-246040 and from Spagnolo et al., 2007 for SB-612111. Receptor binding data are expressed as pK_i, GTPγS binding and BRET data are expressed as pK_B, other data are expressed as pA_2.

JPET Fast Forward. Published on January 14, 2020 as DOI: 10.1124/jpet.119.262865
This article has not been copyedited and formatted. The final version may differ from this version.

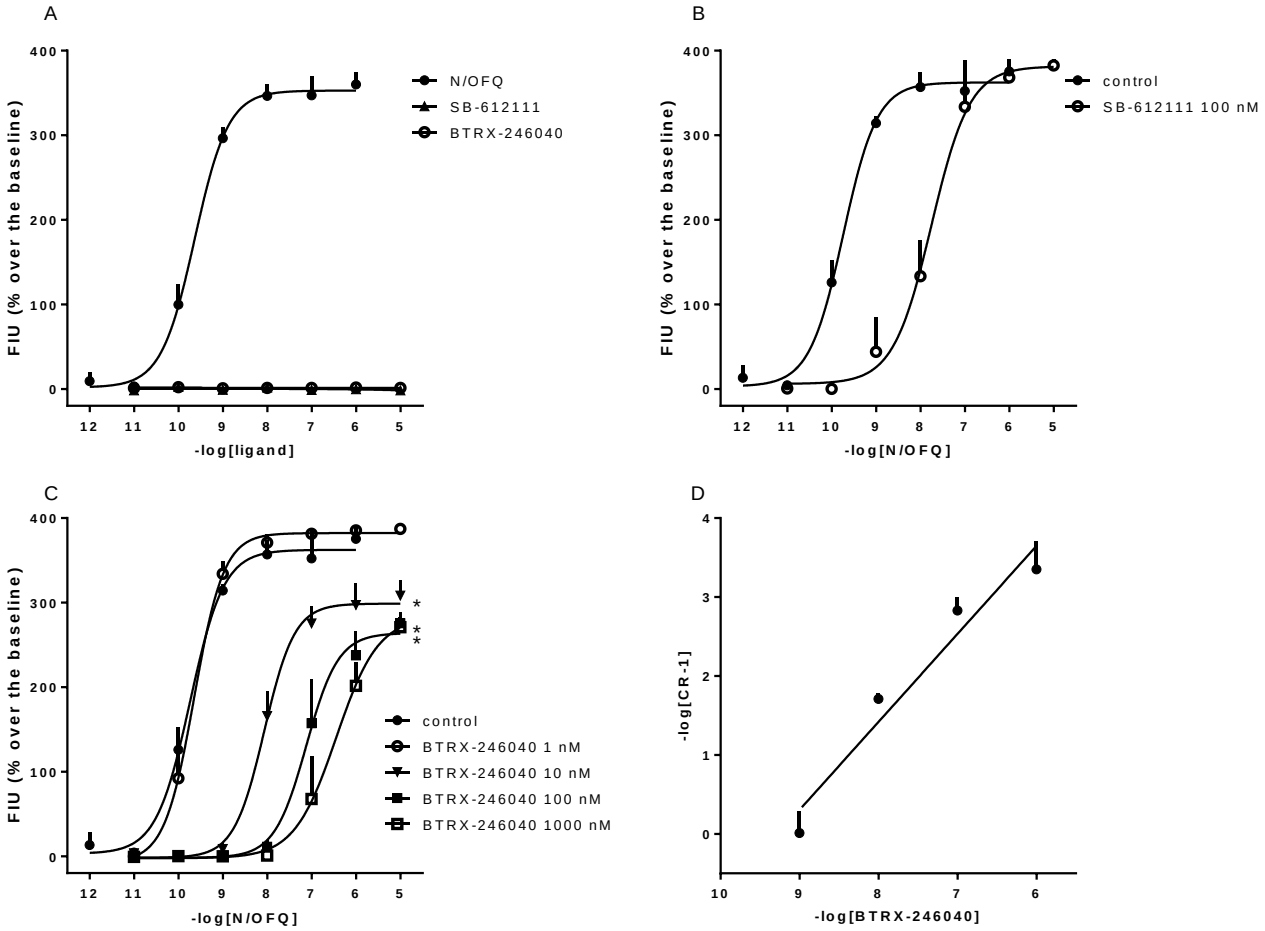

Figure 1

JPET Fast Forward. Published on January 14, 2020 as DOI: 10.1124/jpet.119.262865
This article has not been copyedited and formatted. The final version may differ from this version.

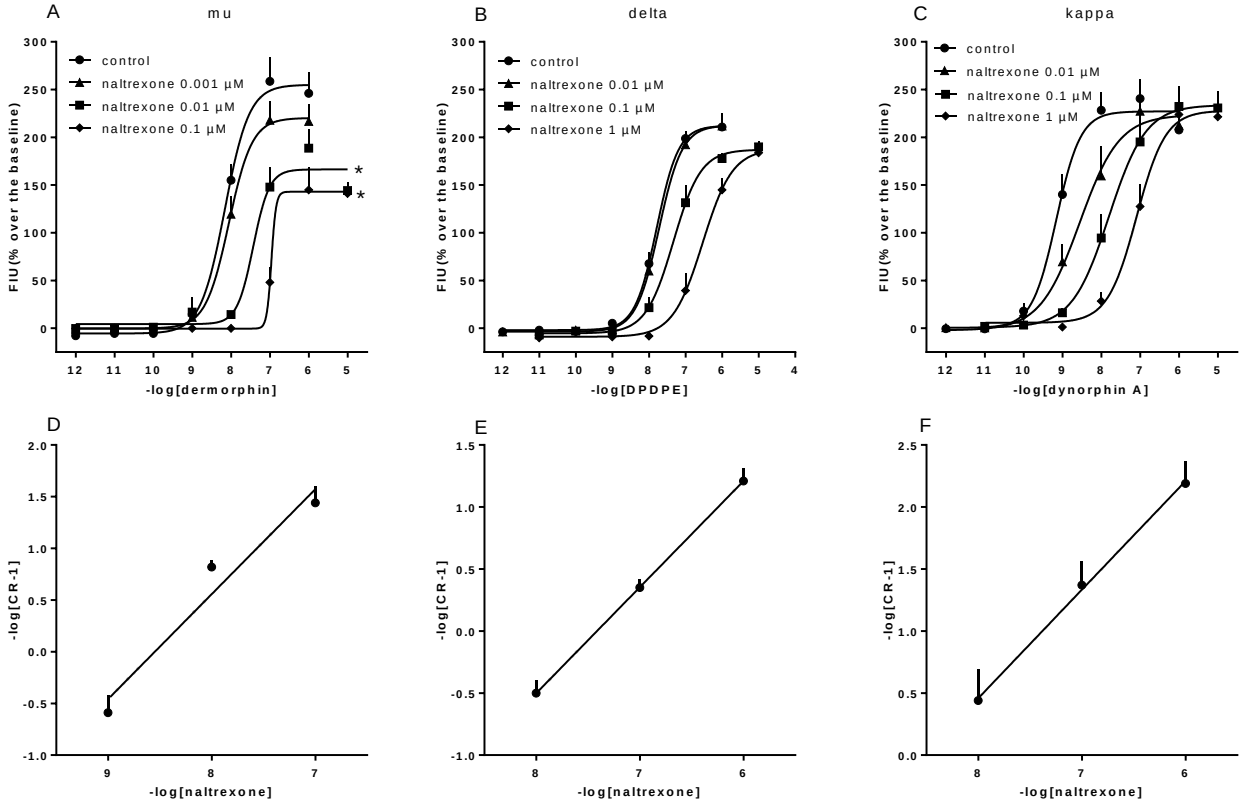

Figure 2

JPET Fast Forward. Published on January 14, 2020 as DOI: 10.1124/jpet.119.262865
This article has not been copyedited and formatted. The final version may differ from this version.

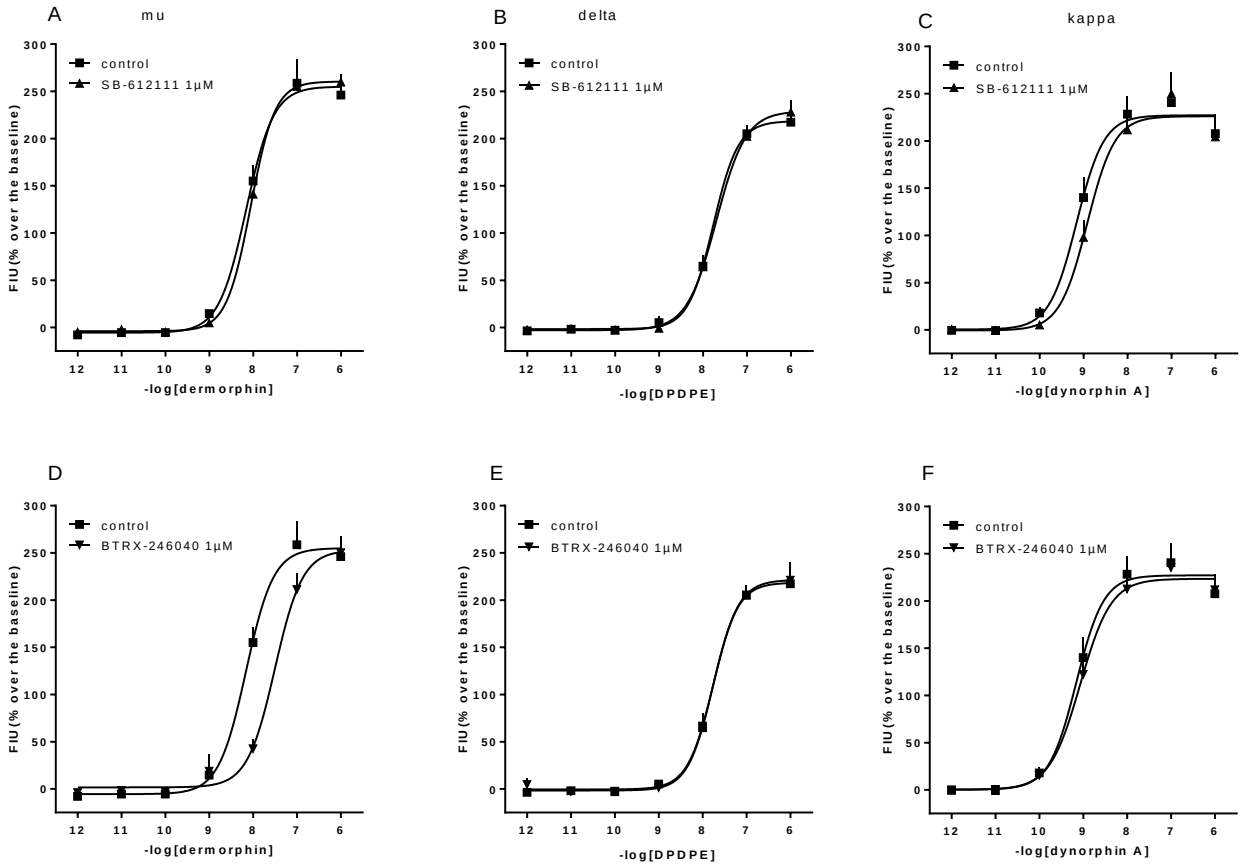

Figure 3

JPET Fast Forward. Published on January 14, 2020 as DOI: 10.1124/jpet.119.262865
This article has not been copyedited and formatted. The final version may differ from this version.

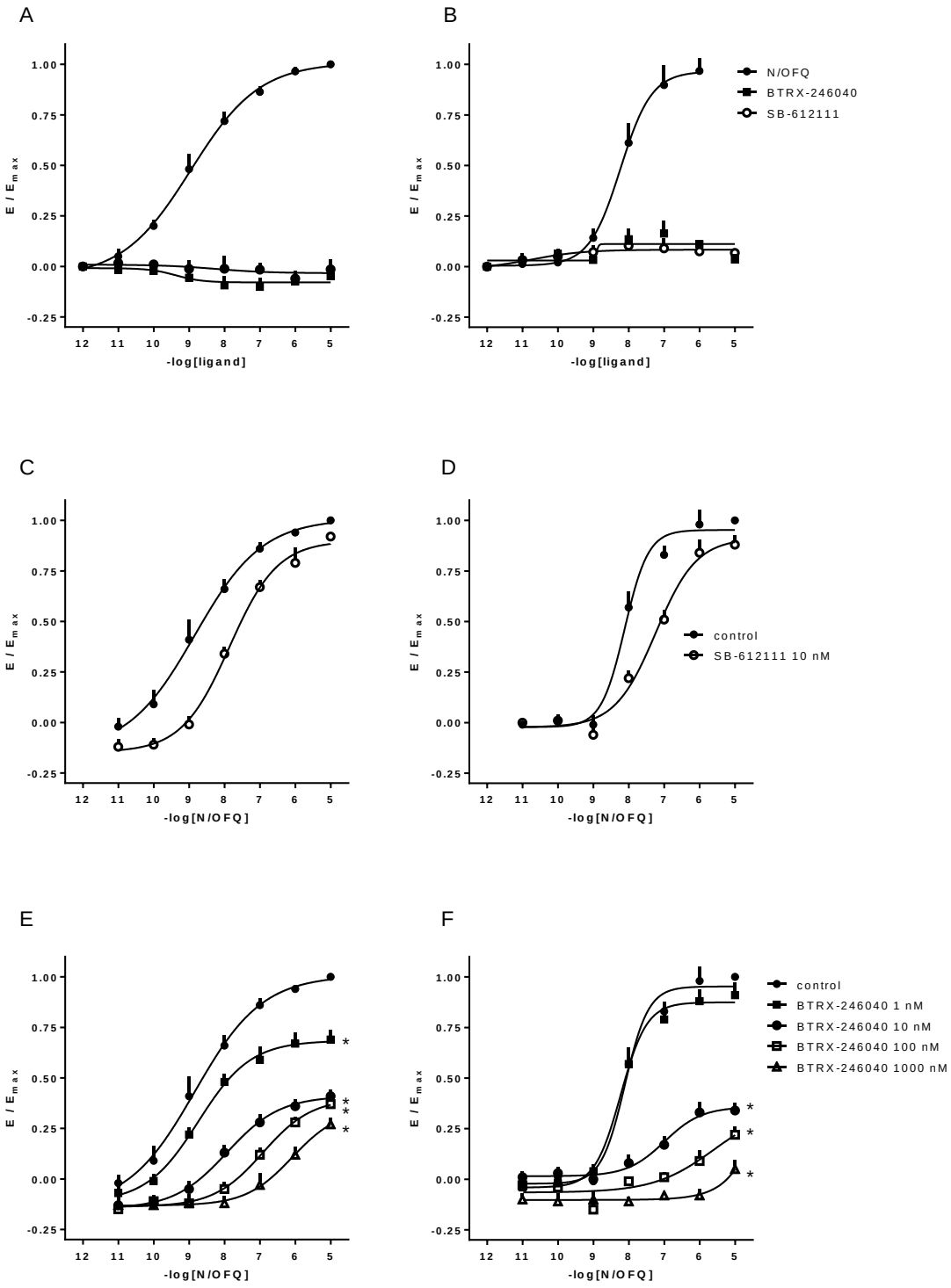

Figure 4

JPET Fast Forward. Published on January 14, 2020 as DOI: 10.1124/jpet.119.262865
This article has not been copyedited and formatted. The final version may differ from this version.

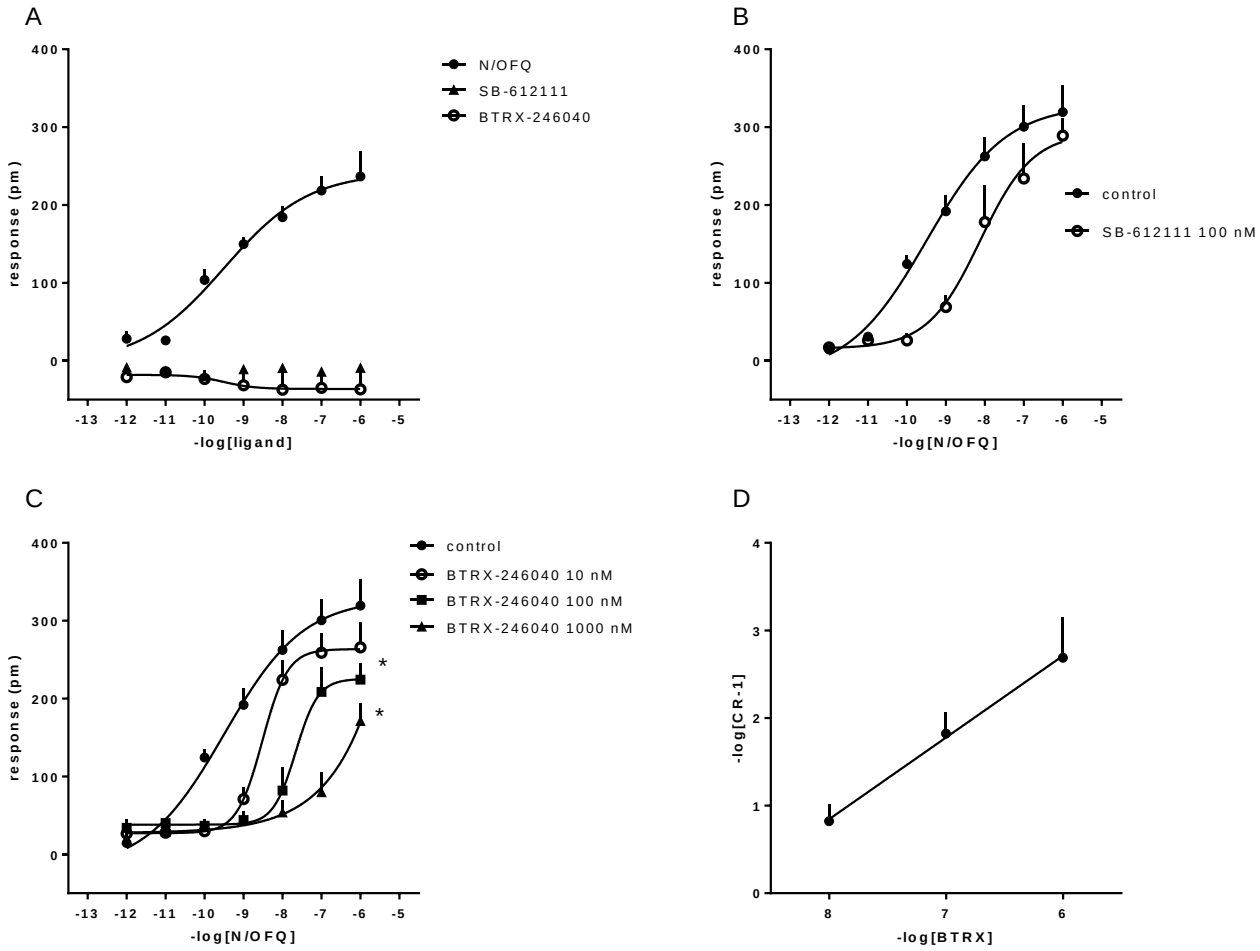

Figure 5

JPET Fast Forward. Published on January 14, 2020 as DOI: 10.1124/jpet.119.262865
This article has not been copyedited and formatted. The final version may differ from this version.

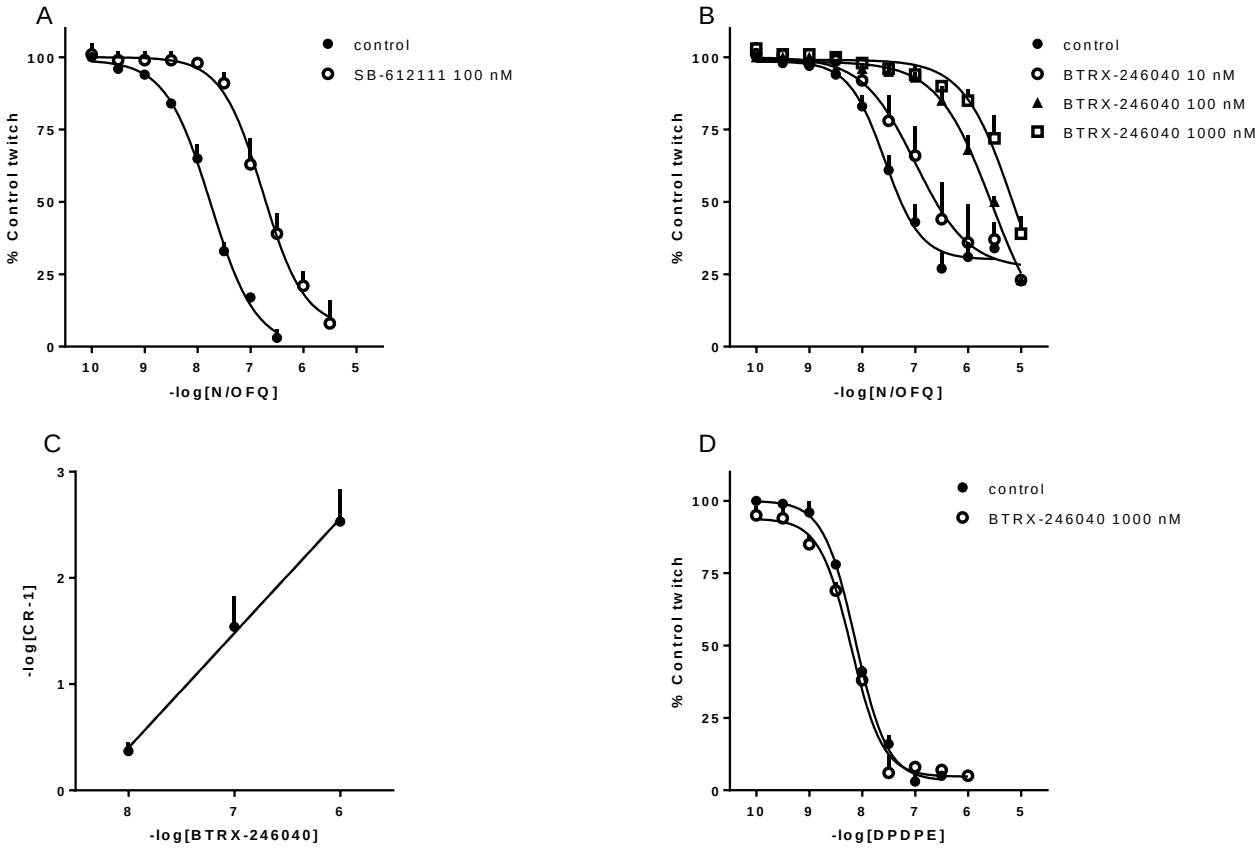

Figure 6